FRACTURE MECHANICS ANALYSIS OF SINGLE FIBER FRAGMENTATION TEST

Ramirez F. A.[1], Acha B.A.[2], and Carlsson L.A.[1]

[1] Department of Mechanical Engineering, Florida Atlantic University
777 Glades Road, Boca Raton, FL 33431, USA

[2] Department of Ocean Engineering, Florida Atlantic University
101 N. Beach Road, Dania Beach, FL 33004, USA

ABSTRACT

A simple fracture mechanics model was developed to quantify the fiber/matrix interface fracture toughness using a modified test procedure for the single fiber fragmentation test (SFFT). The approach considers initially the event of the first fiber break followed by instantaneous fiber/matrix debonding using the typical SFFT procedure. It is realized, however, that determining the interfacial fracture toughness from the instantaneous F/M debonding event can be too complex since this event is dependent of the energy released by the fiber break. In order to separate the fiber fracture and debond propagation events, a modified test procedure was developed. The new procedure consists of unloading and loading the SFFT specimen after the first fiber break and instantaneous F/M debonding are achieved. In this way the energy release rate for debond propagation can be determined independently of other fracture processes. The modified SFFT procedure was performed on E-glass/vinylester specimens to illustrate the applicability of the fracture mechanics model proposed in this analysis. The fracture toughness value obtained for this system, G_{cd} =62 J/m^2, is in agreement with toughness values obtained by other authors for similar systems.

1. INTRODUCTION

The structural integrity and lifetime of polymer composites are critically dependent on the stability of the fiber/matrix (F/M) interface region [1,2]. Therefore, it is extremely important to characterize the F/M interface to understand the overall performance of polymer matrix composites.

Among the test methods to evaluate the bonding between fiber and matrix, the single fiber fragmentation test (SFFT) method is the simplest in terms of the experimental setup, and therefore commonly used [2]. The SFFT consists of a single fiber embedded in a resin matrix molded into a dog-bone specimen. The specimen is tested in tension and, if the specimen is properly designed, the fiber will break into several fragments until fiber break saturation occurs. The final fragmentation length is called *critical length, 'l_c'* [3]. Several models have used the critical length to determine the F/M interface shear strength [3,4]. Typically, the F/M interface shear strength has been estimated from the Kelly-Tyson shear lag analysis [4]. The Kelly-Tyson model, however, is associated with inaccuracies since it assumes a constant shear stress along the F/M interface and does not account for other failure processes that are involved in the fragmentation test. For instance, it has been observed that every fiber break is accompanied by a finite amount of F/M debonding (or instantaneous debonding) [5] and therefore, a fracture toughness quantity such as the energy release rate for propagation of interfacial debonding may be better filled to quantify the F/M interface adhesion than a shear strength parameter. Currently there are several models based on fracture toughness criterion to evaluate the F/M interface [6,7]. These models, however, are very complex because they integrate the effects of energy released by a fiber fracture with debonding propagation.

The aim of this work is to develop a simple fracture mechanics model and test procedure for quantifying the interfacial fracture toughness. Three fundamental fracture events are considered: fiber break, F/M debond initiation, and debond growth. In order to separate the fiber fracture and debond propagation events, a modified single fiber fragmentation test procedure is proposed. The new test procedure consists of unloading the SFFT specimen after the first fiber break and instantaneous F/M debonding are achieved. The SFFT specimen is then loaded again until the existing debond region grows and in this way the energy release rate for debond propagation can be determined independently of the energy released rate by the first fiber fracture. Experiments to illustrate the applicability of the fracture mechanics model developed in this analysis are performed on SFFT specimens consisting of an E-glass fiber and vinylester matrix which are typical materials used in naval applications.

2. FRACTURE MECHANICS MODEL

The fundamental fracture events in the fragmentation test are illustrated in Figure 1.

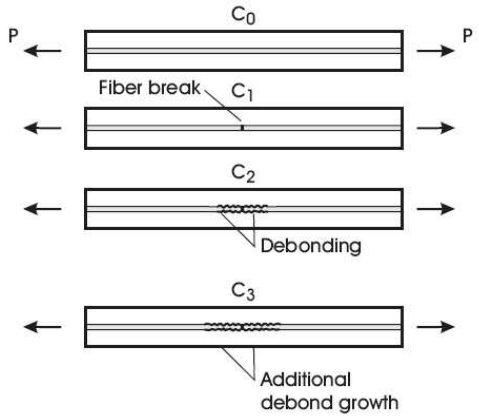

Figure 1: Schematic of fracture events and associated compliance of SFFT specimen.

In the first stage, there is no damage, and the specimen compliance is C_o. After the fiber breaks, the energy release rate by the fiber fracture, G, is determined in terms of the difference in specimen compliance before, C_o, and after the fiber breaks, C_1. In the second fracture stage, it is considered that the excess of released energy by the fiber fracture may generate instantaneous F/M debonding. An expression for G for debonding following a fiber break can be derived in terms of compliance difference between C_2 and C_1 (not derived in this paper). Finally, in the third stage, the SFFT specimen is assumed to be unloaded after the fiber breaks and debonds, and then loaded again until the existing debond starts to grow. The interfacial fracture toughness, G_{cd}, is determined by the difference in specimen compliance (i.e. C_3-C_2) after an existing debond length starts to extend.

In the first stage of this analysis, we will consider only the event of first fiber failure assuming that the fiber/matrix interface remains undamaged. The break is assumed to occur in the center of the specimen enabling consideration of the half symmetry section in Fig. 2. This assumption is not physically reasonable but should be valid for an arbitrary fracture site.

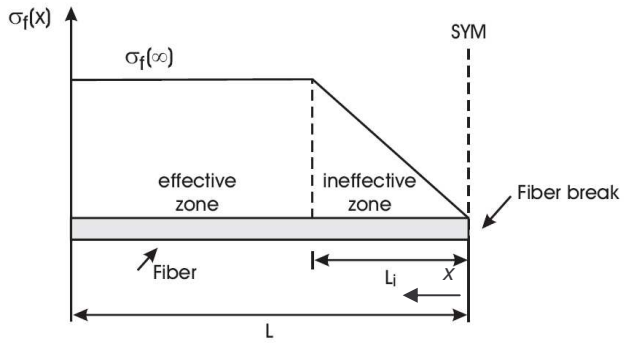

Figure 2. Schematic of fiber stress distribution after a fiber break in a symmetry section of SFFT specimen for the case of no F/M debonding.

The fiber stress distribution around a fiber break is illustrated in Figure 2. After the fiber breaks, it carries no load at the break point. The regions of the broken fiber near the fiber break point are subject to interfacial shear stress which will transfer load from the matrix into the fiber. The zone over which the fiber stress builds up is identified as the *ineffective zone.* The ineffective length, L_i, is the distance required to recover the stress in the fiber to the far-field stress. The zone where the fiber is fully loaded away from the break point is considered as the *effective zone*. The fiber tensile stress distribution in the ineffective length region is given by an axisymetric model developed by Whitney and Drzal [8],

$$\sigma_f(x) = \left[1 - (4.75\frac{x}{L_i} - 1)e^{\left(-4.75\frac{x}{L_i}\right)}\right] A_1 \varepsilon_0 \tag{1}$$

where x is the distance from the fiber break point along the fiber axis ($0 \le x \le L_i$), see Fig. 2. The far-field regions of the fiber and matrix are assumed to be subjected to a uniform axial strain ε_0. A_1 is a material property constant defined as:

$$A_1 = E_{1f} + \frac{4K_f G_m \nu_{1f}}{(K_f + G_m)}\left(\nu_{1f} - \nu_m\right) \tag{2}$$

where

$$K_f = \frac{E_m}{2(2 - E_{2f}/2G_{2f} - 2\nu_{2f}E_{2f}/E_{1f})} \tag{3}$$

E_{1f}, E_{2f}, ν_{1f}, and ν_{2f} are the cylindrical orthotropic fiber axial and transverse moduli and Poisson's ratios respectively, and G_{2f} refers to the shear modulus in the transverse plane of the fiber. E_m and G_m are the Young's and shear modulus of the matrix.

The Whitney-Drzal model provides the following expression for the ineffective length:

$$L_i = \frac{2.375(d_f/2)}{\overline{\mu}} \tag{4}$$

where

$$\overline{\mu} = \sqrt{\frac{G_m}{E_{1f} - 4\nu_{1f}G_m}} \tag{5}$$

To implement a fracture mechanics analysis, the total displacement of the SFFT specimen under tensile loading before and after a fiber break has to be calculated. Before a fiber break, the total specimen displacement, δ_o, is given by Hooke's law as:

$$\delta_o = \frac{2PL}{A_c E_c} \tag{6}$$

where A_c and E_c are the cross section area and effective Young's modulus of the SFFT specimen and P is the axial load

$$A_c = \frac{\pi}{4}(2R)^2 \tag{7}$$

$$E_c = V_f E_{1f} + V_m E_m \tag{8}$$

$$P = \varepsilon_o E_c A_c \tag{9}$$

where R is the radius of the (assumed) cylindrical SFFT specimen. V_f and V_m are the volume fraction of the fiber and matrix calculated as:

$$V_f = \frac{A_f}{A_c} \quad \text{and} \quad V_m = \frac{A_m}{A_c} \tag{10 a,b}$$

where A_f and A_m are the cross section areas of fiber and matrix,

$$A_f = \frac{\pi}{4} d_f^2 \quad \text{and} \quad A_m = A_c - A_f \tag{11 a,b}$$

After a fiber break (see Fig. 2), the total displacement of the SFFT specimen, δ_1, is given by the sum of the displacements of the effective (e) and ineffective (i) regions,

$$\delta_1 = \delta_{1,e} + \delta_{1,i} \tag{12}$$

The displacement in the effective zone is given by:

$$\delta_{1,e} = 2\frac{P(L - L_i)}{A_c E_c} \tag{13}$$

The displacement in the ineffective zone is given by:

$$\delta_{1,i} = 2\int_0^{L_i} \varepsilon(x)dx \tag{14}$$

Where the strain in the ineffective region is:

$$\varepsilon(x) = \frac{\sigma_m(x)}{E_m} \tag{15}$$

σ_m is the matrix stress which may be obtained from equilibrium of force,

$$\varepsilon(x) = \frac{P - \sigma_f(x)A_f}{A_m E_m} \tag{16}$$

Substitution of Eq. (16) into (14) yields:

$$\delta_{1,i} = 2\frac{PL_i}{A_m E_m}\left(1 - \frac{0.591248827 A_f A_1}{A_c E_c}\right) \tag{17}$$

The total displacement of the specimen after the fiber breaks is:

$$\delta_1 = 2\frac{P(L - L_i)}{A_c E_c} + 2\frac{PL_i}{A_m E_m}\left(1 - \frac{0.591248827 A_f A_1}{A_c E_c}\right) \tag{18}$$

The energy release rate, G, for fracturing a fiber in the SFFT specimen is given in terms of compliance,

$$G = \frac{P^2}{2}\frac{\Delta C}{\Delta A} \tag{19}$$

where P is the load required to break the fiber in the SFFT specimen, ΔA is the new surface area created and it is considered as the cross section area of the fiber,

$$\Delta A = \frac{\pi}{4} d_f^2 \tag{20}$$

and ΔC is the difference in the SFFT specimen compliance before and after the fiber break. The SFFT specimen compliance before the fiber break, C_o, is given by:

$$C_o = \frac{\delta_o}{P} = \frac{2L}{A_c E_c} \tag{21}$$

and the SFFT specimen compliance after a fiber break, C_1, is given by:

$$C_1 = \frac{\delta_1}{P} = 2\frac{(L - L_i)}{A_c E_c} + 2\frac{L_i}{A_m E_m}\left(1 - \frac{0.591248827 A_f A_1}{A_c E_c}\right) \tag{22}$$

Hence, the energy release rate when the fiber breaks in the SFFT specimen is given by:

$$G = \frac{4P^2 L_i}{\pi d_f^2}\left(\frac{1}{A_m E_m} - \frac{0.591248827 A_f A_1}{A_c A_m E_c E_m} - \frac{1}{A_c E_c}\right) \tag{23}$$

As mentioned before, the excess of released energy by the fiber fracture will generate instantaneous F/M debonding. If debonding between fiber and matrix follows a fiber break, three zones are considered for F/M debonding analysis as shown in Figure 3 (i.e. the effective zone, the ineffective zone and the debond zone).

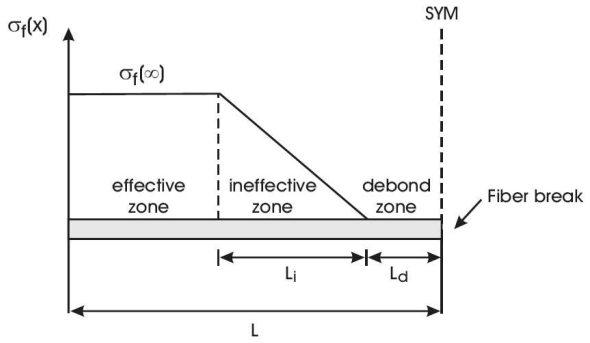

Figure 3: Schematic the fiber stress distribution in a symmetry section of SFFT specimen after a fiber break with F/M debonding.

In this stage of the analysis, an expression for the interfacial fracture toughness, G_{cd}, is derived based in the event of debond growth, see Fig. 1 ($C_3 \rightarrow C_2$). In order to separate the influence of the energy released by the fiber fracture on debond propagation, the SFFT specimen is unloaded after a fiber break and instantaneous debonding are achieved. Then the specimen is loaded again until the existing debond length extends. The energy release rate by debond propagation, G_d, is determined by the difference in compliance, (i.e. C_3-C_2), after an existing debond length extends.

The displacement of the specimen containing a fiber break and instantaneous debonding is given by:

$$\delta_2 = \delta_{2,e} + \delta_{2,i} + \delta_{2,d} \tag{24}$$

where the displacement at the effective region, $\delta_{2,e}$, is given by:

$$\delta_{2,e} = 2\frac{P\left(L - L_i - L_d\right)}{A_c E_c} \tag{25}$$

The displacement at the ineffective region, $\delta_{2,i}$, is obtained from Eq. (18)

$$\delta_{2,i} = \delta_{1,i} = 2\frac{PL_i}{A_m E_m}\left(1 - \frac{0.591248827 A_f A_1}{A_c E_c}\right) \tag{26}$$

and the displacement at the debond region is given by:

$$\delta_{2,d} = 2\frac{PL_d}{A_c E_d} \tag{27}$$

where the effective modulus of the debond region is:

$$E_d = V_m E_m \tag{28}$$

The compliance of the SFFT specimen after instantaneous debonding is:

$$C_2 = \frac{\delta_2}{P} = 2\frac{(L - L_i - L_d)}{A_c E_c} + 2\frac{L_i}{A_m E_m}\left(1 - \frac{0.591248827 A_f A_1}{A_c E_c}\right) + 2\frac{L_d}{A_c E_d} \tag{29}$$

When the SFFT specimen is loaded again (after unloaded at fiber failure and instantaneous debonding stage), the existing debond length will start to extend at a critical load, P_c. If the F/M debonding length extends an increment $d(L_d)$, the effective length will decrease by $d(L_d)$ (at each side of the fiber break point), see Fig.3. Therefore, the SFFT specimen compliance after debond propagation, C_3, is given by:

$$C_3 = 2\frac{(L - L_i - L_d - dL_d)}{A_c E_c} + 2\frac{L_i}{A_m E_m}\left(1 - \frac{0.591248827 A_f A_1}{A_c E_c}\right) + 2\frac{L_d + dL_d}{A_c E_d} \tag{30}$$

The difference in compliance is:

$$\Delta C = C_3 - C_2 = 2dL_d\left(\frac{1}{A_c E_d} - \frac{1}{A_c E_c}\right) \tag{31}$$

and the increment in debond area is given by:

$$\Delta A = \pi d_f \left(2dL_d\right) \tag{32}$$

The energy release rate by debond propagation is then,

$$G_d = \frac{P^2}{2\pi d_f}\left(\frac{1}{A_c E_d} - \frac{1}{A_c E_c}\right) \tag{33}$$

From the facture criterion, the existing debond length will start propagating when G_d is equal to the interfacial fracture toughness, G_{cd}. Therefore, the interfacial fracture toughness is given by:

$$G_{cd} = \frac{P_c^2}{2}\frac{\Delta C}{\Delta A} = \frac{P_c^2}{2\pi d_f}\left(\frac{1}{A_c E_d} - \frac{1}{A_c E_c}\right) \tag{34}$$

Equation (34) reveals that G_{cd} does not depend on the debond length. Hence, the single fiber fragmentation test should produce stable F/M debond propagation.

3. EXPERIMENTAL

3.1 Materials and specimens

The experiment was performed on the single fiber fragmentation test specimen shown in Fig. 4 consisting of an E-glass fiber and vinylester Derakane 8084 (VE D8084) matrix. The properties of fiber and matrix are listed in Table 1.

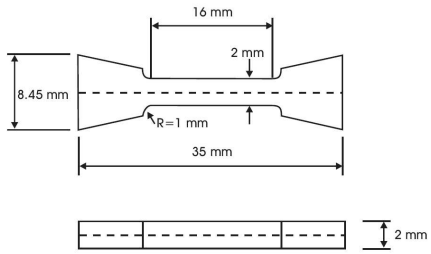

Figure 4: Single fiber fragmentation test (SFFT) specimen [9].

Table 1: Mechanical properties of E-glass fiber and vinylester matrix.

Fiber	Axial modulus, E_{1f}	*(GPa)*	73
	Transverse modulus, E_{2f}	*(GPa)*	73
	Axial Poisson's ratio, v_{1f}		0.2
	Strain to failure, ε	*(%)*	8-10
	Fiber fracture toughness, Γ_f	(J/m^2)	10 [10]
	Diameter, d_f	*(μm)*	14
Matrix	Young's modulus, E_m	*(GPa)*	2.7
	Poisson's ratio, v_m		0.34

3.2 Test Procedure

The SFFT specimen is loaded in tension using a small tensile stage. The fiber fracture and F/M debonding are examined during SFFT testing using photoelastic patterns observed in optical transmission microscopy (Olympus BX41 with a QICAM-FAST 1394 camera). The region around a fiber break exhibits a colored pattern called birefringence. This phenomenon is caused by shear stresses in the matrix [11]. Figure 5 shows a schematic of the birefringence patterns around a fiber break

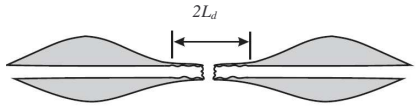

Figure 5: Schematic feature of photoelastic patterns around a fiber break.

The first part of the experiment consists in loading the SFFT specimen in tension until the fiber breaks. The load required, P, to break the fiber is recorded. The instantaneous debond length created by the energy released in this event is measured and it is used as a reference to later study debond propagation. Then, the SFFT specimen is unloaded, and loaded again until the existing debond length increases. The load required to extend the debond, P_c, is recorded.

4. RESULTS AND DISCUSSION

Ten replicate E-glass/vinylester SFFT specimens were tested. The specimens were loaded in tension until reaching a fiber break. Figure 6 shows a typical birefringence pattern at the first fiber break which occurred at 2.1% strain. The strain is calculated from the applied load, P, using the expression: $\varepsilon = P/(A_c E_c)$. This calculation assumes linear-elastic response. Some of the higher strains encountered were beyond the proportional strain limit of the matrix [12], but the deviation from linearity was quite small.

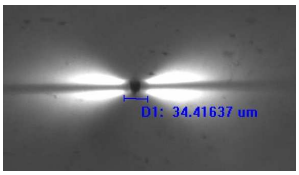

ε_o= 2.1%

Figure 6: Birefringence pattern of the first fiber break in a SFFT specimen.

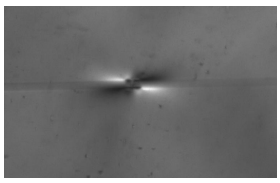

Figure 7: Fiber break point at external loading released state.

After determining the load and the length of the instantaneous fiber/matrix debond region, $2L_d$, at the fiber fracture event, the SFFT specimen was unloaded. Figure 7 illustrates the region near the fiber break point when the external load was removed. Even though the birefringence patterns partially disappeared after unloading the SFFT specimen, there was still evidence showing that the fiber/matrix interface was damaged by the energy released at fiber fracture.

The SFFT specimen was loaded again and the fiber/matrix debond length at the first fiber break was measured at different applied strains. Figure 8 shows the birefringence effects near the fiber break as the externally applied strain was increased. It is evident that at certain critical strain (load), the existing debond length start to propagate.

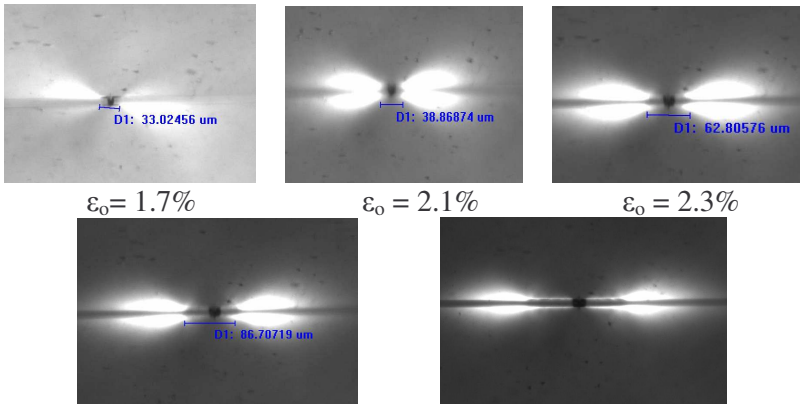

ε_o= 1.7% ε_o = 2.1% ε_o = 2.3%

ε_o = 2.4% ε_o = 2.7%

Figure 8: Fiber/matrix interface debond growth.

4.1 Determination of Debond Fracture Toughness

The load, P, required to break the E-glass fiber in the SFFT specimen was determined to be 237 $\pm$ 9 N. The energy release rate, G, corresponding to the fiber failure load is 2040 $\pm$ 437 J/m^2 (Eq. (23)). (Nairn reported that the energy released rate during fragmentation of T50 carbon fibers is around 4600J/m^2 [6] which is in reasonable proportion to the value reported here for E-glass fibers). A small portion of this released energy actually

goes into fracturing the fiber (it has been found that the toughness of a glass fiber is only around 10 J/m^2 [9]), while part of the remaining energy is responsible for the instantaneous F/M debonding observed [6].

Figure 9 depicts the length, $2L_d$, of the debonded region near a fiber break vs. applied strain for specimens that were previously unloaded after first fiber fracture.

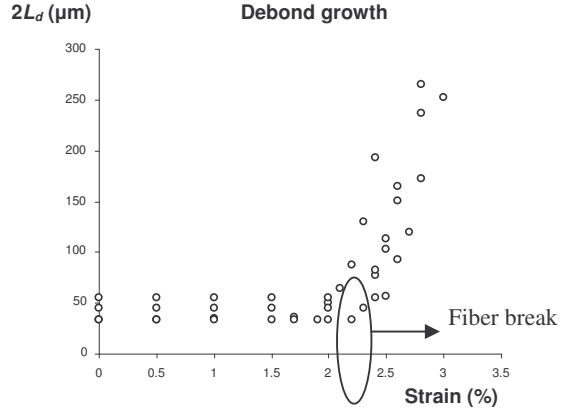

Figure 9: Debond length growth as a function of applied strain.

From Figures 8 and 9, it can be deduced that, for this composite system, the existing debond length starts to propagate at an external load, P_c, approximately equal to the load required to break the fiber. Furthermore, the energy release rate required to grow an existing debond (or interfacial fracture toughness, G_{cd}) determined from Eq. (34) is 62 $\pm$ 13 J/m^2. The energy required for debond propagation has been estimated using pull-out experiments by Di Francia et al. [13]. They reported a fracture toughness, G_{cd}, of 50 J/m^2 for glass/epoxy which is comparable to the fracture toughness (62 J/m^2) found in this research for a glass/vinylester system.

It must be point out that this model does not account for the presence of friction at the interface. A more rigorous analysis including frictional shear stress acting over the debonded region is currently been developed.

5. CONCLUSIONS

The objective of this paper was to develop a test methodology and a simple fracture mechanics model for determining the toughness of the fiber/matrix interface by means of the single fiber fragmentation tests. It has been realized by other authors [6] that the energy consumed by fracturing the fiber in the SFFT specimen is much less than the energy available in the SFFT specimen at the point of fiber fracture. The remaining energy is consumed in other processes such as instantaneous F/M debonding. Determining an interfacial fracture toughness from the instantaneous F/M debonding event can be too complex since this event is dependent of the energy released by the fiber break. Therefore, a modified SFFT procedure was designed to determine the interfacial fracture toughness by separating the events of fiber break and instantaneous debonding from the event of debond growth. The new SFFT procedure consists of unloading the specimen after the first fiber break and instantaneous F/M debonding are achieved. The specimen is then loaded again until the existing debond region grows. The critical load required to initiate debond propagation is then recorded and the energy

release rate for debond growth can be determined independently of the energy released rate by the fiber fracture. This procedure was performed on E-glass/vinylester specimens to illustrate the applicability of the model. The fracture toughness value determined in this paper, G_{cd} = 62 J/m^2, is in reasonable agreement with results obtained for glass/epoxy by other investigators [13].

ACKNOWLEDGEMENTS

The authors acknowledge support for this work at Florida Atlantic University from ONR grant No. N00014-05-1-0341 managed by Dr. Yapa Rajapakse. Thanks are due to Shawn Pennell for the art work.

REFERENCES

1. Ray, B.C., "Temperature Effect During Humid Ageing on Interfaces of Glass and Carbon Fibers Reinforced Epoxy Composites" *Journal of Colloid and Interface Science,* 2006, 298: 111-117.
2. Rao, V., Herra-Franco, P.J., Ozzelo, A.D., Drzal, L.T. "A Direct Comparison of the Fragmentation Test and the Microcond Pull-out Test for Determining the Interfacial Shear Strength" *The Journal of Adhesion,* 1991,34:65-77.
3. Drzal, L.T, Rich, M.J., Camping, J.D., Park, W.J., "Interfacial Shear Strength and Failure Mechanisms in Graphite Fiber Composites" *35th Annual Reinforced Plastics/Composites Conference*, Paper 20C, 1980
4. Kelly. A., Tyson, W.R.,"Tensile Properties of Fiber-Reinforced Metals: Copper/Tungsten and Copper/Molybdenum" *Journal of the Mech. and Phys. of Solids*, 1965, 13, 329-350,
5. Kim B.W., Nairn J.A., "Experimental Verification of the Effects of Friction and Residual Stress on the Analysis of Interfacial dDbonding and Toughness in Single Fiber Composites", *Journal of material Science*, 2002, 37: 3965 – 3972.
6. Nairn J.A., Liu Y.C.,"On the Use of Energy Methods for Interpretation of Results of Single-Fiber Fragmentation Experiments", *Composite Interfaces,* 1996, 4:241-267.
7. Wagner H. D, Nairn J. A. and Deteassis, "Toughness of Interfaces from Initial Fiber-Matrix Debonding in a Single Fiber Composite Fragmentation" *Applied Composite Materials, 1995,* 2: 107-117.
8. Whitney J.M., Drzal L.T., "Axisymmetric Stress Distribution Around An Isolated Fiber Fragment", *ASTM Special Technical Publication*, 1987, 179-196.
9. Feih, S., Wonsyld, K., Minzari, D., Westmann, P. and Liholt, H., "Testing Procedure for the Single Fiber Fragmentation Test', *Riso National Laboratory*, Riso-R- 1483(EN), Roskilde, Denmark, 2004.
10. Harris, B., Morley, J., Phillips, D.C., "Fracture Mechanism in Glass-Reinforced Plastics", *Journal of Material Science*, 1975, 10:2050
11. Timoshenko, S., "Theory of Elasticity" McGraw-Hill, 1934.
12. Ramirez, F.A., Carlsson, L.A., Acha, B.A., "Evaluation of Environmental Effects on Polymer Matrix Composites by Micromechanical and Macromechanical Tests", *13th European Conference on Composite Materials,* 2008
13. Francia, C.D., Ward, T.C., Claus, R.O., "The Single Fibre Pull-Out Test 1: Review and Interpretation", *Composites: Part A*, 1996, 27A:591-612